JOURNAL OF COMPUTATIONAL PHYSICS 4, 195–203 (1969)

Computation and Analysis of Pulsed-NMR Line Shapes of Crystals*

MARCEL KOPP†

Mellon Institute, Carnegie-Mellon University, Pittsburgh, Pennsylvania 15213

Received August 20, 1968

ABSTRACT

Programs are described that compute and analyse the decay shape of the free-precession signal envelope (lattice sums and Fourier transforms). Applications to CaF_2, gypsum, H_2S and ice are reported. Comparisons of calculation and analysis allow deductions about the disposition of the spins on the lattice.

PURPOSE

One may calculate the absorption spectrum of a spin system by diagonalizing its hamiltonian; but for a crystal of spins $\frac{1}{2}$ (strictly dipolar broadening) the large number of interacting spins to be considered makes the hamiltonian matrix too large ($2^n \times 2^n$ for n spins). One can however calculate to a reasonable approximation the Fourier transform of the spectrum. This is the decay shape of the free-precession signal-envelope, which is the response of the system to a powerful pulsed irradiation at the resonance frequency. The method was successful [1, 2] for reproducing the shapes of fluorite (CaF_2), a simple-cubic array of spins where drastic simplifications are permitted [1]. We have applied the formula of Lowe and Norberg [1] (LN) and that of Evans and Powles [2] (EP) to lattices containing up to 81 spins where no symmetry is required. The early decays coincide for both formulations; however, the later behavior diverges for LN (without an additional farther-neighbor attenuation) but converges for EP. In the latter case, a Fourier transformation to the absorption shape is successful.

Experimentally, the precision of broad-line absorption spectroscopy is impaired by the necessarily large field-modulation, and often by a slow spin-lattice relaxation. Pulse spectroscopy is free from these handicaps, but the observed trace $V(t)$ must

* This work originated while the author was a Visitor with the Department of Physics, and the Crystallography Laboratory, University of Pittsburgh (1965–1967).

† Present address: Westinghouse Research Laboratories, Churchill, Pennsylvania 15235.

581/4/2-4

be corrected to the decay shape $F(t)$, because of delays characteristic of the receiver circuit and coherent detector [3]. The correction is simple, but still the early decay shape (where all spectral moments are contained) is obscured by an instrumental blocking time [4]. The available corrected decay shape must therefore be extrapolated to time origin. A convolution analysis (decomposing the decay as a product of simple functions) was suggested by Abragam [5], and applied to some well-behaved shapes in order to deduce second moments [6, 7]. But, in general, the fit of an even polynomial of high degree (e.g., 20th) to the available decay is more appropriate and successful. Once the decay shape is completed to time origin, it can be Fourier-transformed into the absorption shape. We have thus analyzed numerically the experimental decay shapes of Barnaal [7] for fluorite and ice.

Comparisons between experimental and calculated decay shapes allow deductions about the disposition of the spins on the lattice that are much more significant than second-moment considerations. This information is especially useful for molecular crystals containing hydrogen nuclei, whose positions are frequently left undetermined by X-ray, electron, or even neutron diffraction studies. The aim of the present program development was primarily to determine what structural information can be derived about the intra- and intermolecular configurations in ice from its NMR line shapes [8]. The methods were tested on fluorite (CaF_2), a simple-cubic spin lattice, and on gypsum ($CaSO_4 \cdot 2H_2O$) and hydrogen sulphide (H_2S), simple hydrates; they may be applied to other suitable hydrates or molecular crystals.

Method

Several computer programs have been developed for the pulsed-NMR laboratory [9]. They form two groups:

(A) The calculation of the shape of the free-precession signal envelope, and its graphic display,

(B) the analysis of the experimental free-induction decay trace, and its graphic display.

Group A: Calculations

Program CARTCORD. Given the unit-cell parameters, or those of a Bravais pattern, CARTCORD generates the cartesian coordinates of all the atoms (or spin sites) in the central cell and all desired neighbor cells. It may also serve to generate maps of parallel sections through a ball model of the lattice, or an oblique view of the unit cell.

Program NMR SECMO. Given the coordinates of all spin sites to be considered (the j nonequivalent central sites, and all the neighbors k in successive spherical

shells), and the direction of the magnetic axis $\mathbf{B}_0$ in the *xyz*-frame, NMR SECMO calculates the NMR absorption lineshape second moment, according to Van Vleck's formula [5]:

$$\overline{M}_2 = \langle M_2^{(j)} \rangle_j = \left\langle \sum_k^N S_{jk}^2 \right\rangle_j \tag{1}$$

where

$$S_{jk} = \sqrt{\tfrac{1}{3}(\gamma^2\hbar)^2 I(I+1)}\ \tfrac{3}{2}\{1 - 3\cos^2\theta[\mathbf{B}_0, \mathbf{r}_{jk}]\}/r_{jk}^3 \tag{2}$$

Program NMR DECAY. Given the coordinates to be considered, NMR DECAY calculates the decay shape of the free-precession signal envelope, using either the four-term power-series expansion of Lowe and Norberg [1] (LN) or the two-term Dyson expansion of Evans and Powles [2] (EP). The two solutions coincide for short decay times. For large times, the LN solution diverges, as it is a series in powers of the time.[1] The EP solution converges for large times, but the neglected terms of the Dyson expansion would produce somewhat larger amplitudes in the late decay. Both program versions apply only to spins $\frac{1}{2}$, but they do not require any symmetry for the disposition of the spins. Their computation time requirements are comparable.

NMR DECAY 1 (*LOWE*) evaluates the general formula of LN (Eq. 54), but rewritten in a more convenient form:

$$\begin{aligned} F(t) = \langle F_j(t) \rangle_j &= \sum_{n=0}^{\infty} \langle F_j^{(n)} \rangle_j \frac{t^n}{n!} \\ &\cong \frac{1}{N}\left\{ \sum_j^N F_j^{(0)} - \sum_j^N F_j^{(2)} \frac{t^2}{2!} + \sum_j^N F_j^{(3)} \frac{t^3}{3!} - \sum_j^N F_j^{(4)} \frac{t^4}{4!} \right\} \end{aligned} \tag{3}$$

with

$$\left.\begin{aligned} F_j^{(0)} &= \prod_{a \neq j} \cos(S_{ja}t) \equiv U(t), \qquad F_j^{(1)} \equiv 0 && \text{(Ref. } j\text{)} \\ F_j^{(2)} &= \prod_{a \neq j,k,l} \cos(S_{ja}t) \sum_{l \neq k \neq j} \sum G_{jkl}^{(2)} \sin(S_{jk}t) \sin(S_{jl}t) && \text{(Ref. } j\text{)} \\ F_j^{(3)} &= \sum_{l \neq k \neq j} \sum G_{jkl}^{(3)} \sin(S_{kl}t) \prod_{a \neq k,l} \cos(S_{la}t) && \text{(Ref. } l\text{)} \\ F_j^{(4)} &= \sum_{l \neq k \neq j} \sum G_{jkl}^{(4)} \prod_{a \neq k} \cos(S_{ka}t) && \text{(Ref. } k\text{)} \end{aligned}\right\} \tag{4}$$

[1] This defect may be palliated by multiplying the solution with a gaussian having the same second-moment contribution as the farther spins, or by factoring out the first term $U(t)$ of the expansion and calculating it for a larger sphere than for the other terms.

and

$$\left.\begin{aligned} G^{(2)}_{jkl} &= R_{jk}(S_{kl} - S_{lj}) \\ G^{(3)}_{jkl} &= (R_{lj} + 2R_{jk})\, G^{(2)}_{jkl} - G^{(2)}_{ljk}(2R_{lj} + R_{jk}) \\ &\quad - G^{(2)}_{klj}([S_{lj} - R_{lj}] - [S_{jk} - R_{jk}]) \\ G^{(4)}_{jkl} &= 3[G^{(2)}_{jkl} + G^{(2)}_{jlk}]^2 \end{aligned}\right\} \tag{5}$$

In the notation of LN: $S_{jk} = \frac{1}{2}B_{jk}/\hbar$ and $R_{jk} = \frac{1}{2}A_{jk}/\hbar$. In the case of spins $\frac{1}{2}$ only, $R_{jk} = -\frac{1}{3}S_{jk}$. S_{jk} and R_{jk} are the elemental decay rates caused by the i–k interaction. S_{jk} is also the root-second-moment contribution (as from Eq. 2, but note the sign!); it is also the half-splitting of the resonance line due to the j–k interaction.

NMR DECAY 2(EVANS) evaluates the formula of EP:

$$F(t) = \langle F_j(t)\rangle_j = \frac{1}{N}\sum_j^N \left\{\sum_{n=1}^{\infty} F_j^{(n)}\right\} \tag{6}$$

$$\left.\begin{aligned} F_j^{(0)} &= \prod_{k\neq j} \cos(S_{jk}t) \equiv U(t) \\ F_j^{(1)} &= \frac{1}{3}\sum_{k\neq j} S_{jk}\sin(S_{jk}t) \times P_{jk}t \\ P_{jk} &= \frac{U(t)}{\cos(S_{jk}t)} - \frac{1}{t}\int_0^t \prod_{m\neq j,k} \cos[S_{jm}(t-\tau) + S_{km}\tau]\, d\tau \end{aligned}\right\} \tag{7}$$

Processing of the results. The averaging of Eq. (3) or (6) is to be performed over all the nonequivalent sites in the lattice or, typically, in the unit cell. This task is performed by auxiliary programs: By AVERAG (on the results of NMR DECAY), which also displays a plot of the decay functions, or by AVINFO, which also Fourier-transforms the decay shape into the absorption line shape, or by SPHERAVR, which synthesizes a powder average from the decay results obtained at suitably chosen orientations of the magnetic axis evenly distributed in space (ICOSAHED [10]).

Group B: Analyses

Program FIDANAL. A refined computer program for the analysis of the free-induction decay (f.i.d.) of liquids has been described recently by Ernst and Anderson [11]. The slow time scale of liquid decays makes it unnecessary to correct the experimental results for the instrumental response functions. However, the

decay shapes and corresponding spectra are highly resolved and need a very-fine-mesh analysis. In solids, the decays and spectra are much smoother, but the time scale is comparable with the instrumental lags.

Here, the programmed analysis of the f.i.d. proceeds in four stages:

(1) A progressive least-squares smooth-fit interpolation of the data from the oscilloscope face or from a cumulating device.

(2) Corrections [3] of the observed f.i.d. trace $V(t)$ for the characteristic response times of the receiver circuit, τ_Q, and of the amplifier and coherent detector, τ_D. The free precession decay shape, $F(t)$ is thus obtained:

$$F(t) = V(t) + (\tau_Q + \tau_D)\,\dot{V}(t) + (\tau_Q \times \tau_D)\,\ddot{V}(t).$$

(3) Extrapolation to time origin through polynomial fitting.[2] The pulsed precession decay shape of an NMR line centered at resonance can be described by an alternating series of even powers of the time. One should use as high a degree for the polynomial as is still practical and reasonably limit the fit to about the second zero of the decay shape. The program tests the least-squares fitting to all even polynomials up to one of 38th degree, gives their coefficients, and chooses as the best that polynomial with the most alternating terms. The first, second and third coefficients represent the zero-time amplitude, the second and fourth moments of the absorption shape, respectively.

(4) Finally, the chosen polynomial shape is inserted in place of the missing decay amplitudes at early times. The Fourier cosine transform of the completed shape yields the absorption line shape, which is then integrated to its second and fourth moments for comparison with the values obtained from the polynomial fit.

Applications

(1) *Cartesian coordinates and histograms* are of general utility and have been obtained for various other crystal lattices as well.

(2) *Second moment* contributions of successive shells of neighbors in ice, each weighted with the occupation probability of each site, have been calculated according to the statistical structure of ice (see Fig. 1): Assuming the proton to lie *on* the O–O line and the ration OH/OO to be 0.366(=1.0 Å/2.76 Å), the cumulated second moment converges to 38.9 G² for $\mathbf{B}//c$, and to 33.5 G² for either $\mathbf{B}//a$ or $\mathbf{B}//b$, when 700 sites had been included (sphere radius 11.5 Å). These values approxi-

[2] The program was earlier set up for functional fitting [5–7] by interpolating the experimental zeroes between those of nine broadening functions ranging from forked (doublet) to rounded (gaussian). However, the fits were not as good nor as general as the polynomial fits.

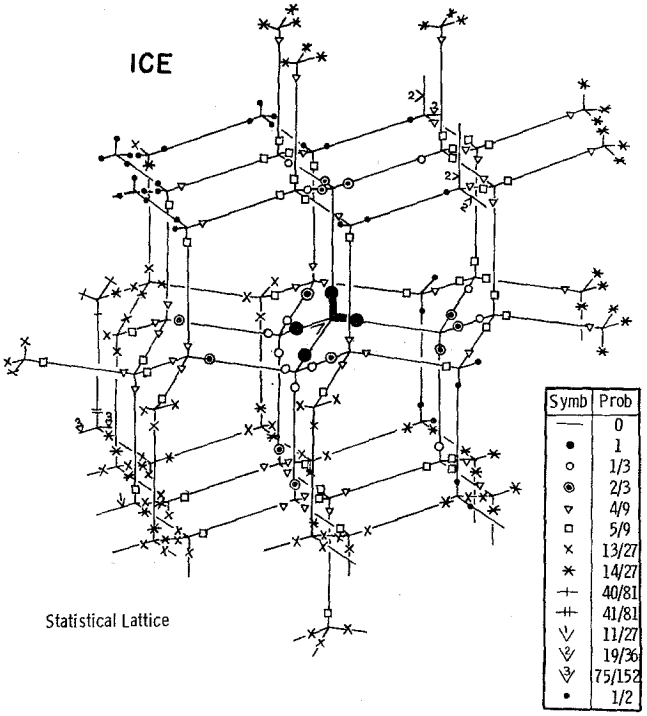

FIG. 1. The statistical lattice of ice. The proton-probability field emanating from a $b \wedge c$ molecule. About a $b \wedge b$ molecule, the probabilities are simply the complements to 1 of those shown here. This figure has also served to evaluate the electrical moment, μ_s, of a cluster of molecules: $\mu_s = 2.33\,\mu$ for 5 molecules, $2.78\,\mu$ for 17, and $3.70\,\mu$ for 50 molecules (μ is the molecular moment).

mate the experimental results of Barnaal [7] and of No. 4 below. Note that, if OH where 4% shorter (0.96 Å as in H_2O vapor), the second moment would be about $6 \times 4\% = 24\%$ larger. Note also that the effects of molecular vibrations and librations approximately cancel each other.

(3) *Decay shape calculations* were made for single-crystal orientations and powder averages of fluorite, gypsum, hydrogen sulphide[3], and H_2O-ice. The results are shown for the case of ice as example in Fig. 2 (EP solutions). The calculations

[3] The powder synthesis for H_2S III by SPHERAVR, using the lattice model of Look and Lowe, [6] predicts the crossover to be at 21.5 μsec, instead of 26 μsec experimentally [6]. Consequently, the HH separation must be about 1.97 Å, i.e., 3.5% larger than in the gas phase. Also, single-crystal data [12] show much less variation of the crossover point than calculated from the model: There should be two molecular orientations, rather than one as assumed by the model.

for ice involve averaging over a set of lattice configurations properly representing the statistical lattice: 6 nonequivalent molecular orientations, 18 possible configurations of the molecule and its six nearest protons. The calculated decay shapes approximate the experimental results [7]. However, the crossover for **B**//c is found earlier than calculated; consequently, the HH separation must be smaller than the value 1.65 Å expected from a tetrahedral $\widehat{HOH}$ angle [8]. The shape for **B**//a shows a flattening before the crossover; but the experimental amplitude is significantly larger than calculated. This feature might be of great interest if short-range preferential ordering could be deduced.

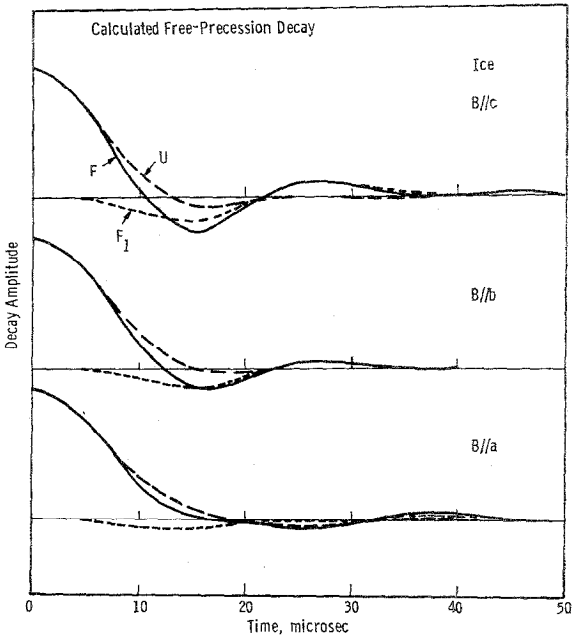

FIG. 2. The calculated free-precession decay shapes of ice (Evans–Powles solution). These are also the correlation functions of cosine waves emitted at every part of the absorption spectrum. $U(t)$ is the first term of the LN- and EP-expansions; it is also the convolution result of successive spin-spin interactions; it quickly loses intensity. $F_1(t)$ is the correction term of the EP–Dyson expansion and arises from the flip-flop conservation of energy; it keeps intensity long after $U(t)$ has decayed. $F(t)$ is the complete free-precession decay shape. The curves shown were obtained by superposing the results of 18 statistical configurations of 53 protons, for field directions along the c-axis, and the three b-axes, and a-axes.

(4) *Decay shape analyses* were performed on the experimental data of Barnaal [7] for fluorite and ice. The results for ice are shown in Fig. 3. (The resulting small

oscillations in the absorption shapes can be due either to truncation of the decay before it has reached negligible intensity or to inaccurate positioning of the base line of the decay shape.) The second-moment values yielded by the polynomial extrapolation are $(12.7 \pm 0.5)G^2$ for CaF_2 **B**//100, $(36 \pm 3)G^2$ for ice **B**//*c*, $(32 \pm 3)G^2$ for ice **B**//*b*, $(28 \pm 3)G^2$ for ice **B**//*a*, and $(30 \pm 3)G^2$ for polycrystalline ice.

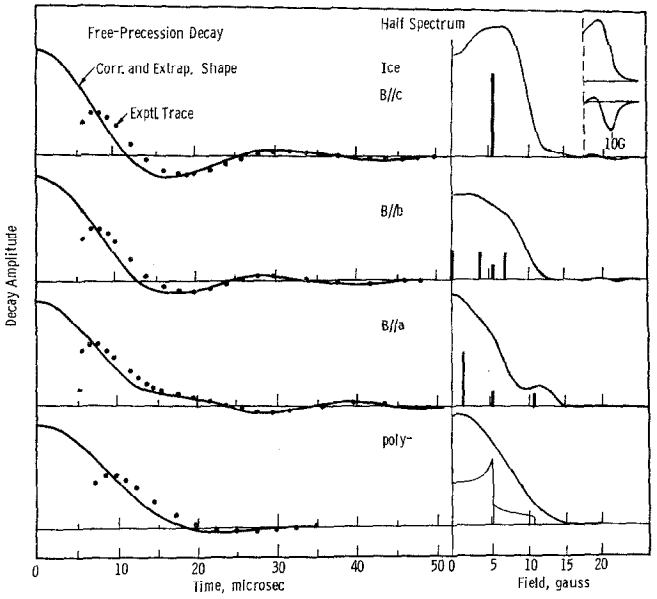

FIG. 3. Analysis of the experimental free-induction decay trace toward the free-precession decay shape and the absorption spectrum. The experimental traces of Barnaal (Ref. [7]) are shown by dots. The experimental absorption spectrum of Ipsen (see G. J. Krüger, Diss., T. H. München, 1961) and the absorption derivative of Kume and Hoshino (*J. Phys. Soc. Japan* **16**, 290, 1961) are shown as insets at upper right. The discrete patterns inside the absorption spectra represent the intra-molecular resonance lines, based on a splitting constant of 5.25G. The correction and extrapolation methods are explained in the text. The half-spectrum is the Fourier transform of the decay shape.

ACKNOWLEDGMENTS

I am grateful to the Physics Department, the Crystallography Laboratory and Mellon Institute for their hospitality, and to the National Science Foundation for covering the computation costs.

REFERENCES

1. I. J. LOWE and R. E. NORBERG, *Phys. Rev.* **107**, 46 (1957); S. CLOUGH and I. R. MCDONALD, *Proc. Phys. Soc.* **86**, 833 (1965); S. GADE and I. J. LOWE, *Phys. Rev.* **148**, 382 (1966).
2. W. A. B. EVANS and J. G. POWLES, *Phys. Letters* **24A**, 218 (1967).
3. D. E. BARNAAL and I. J. LOWE, *Rev. Sci. Instr.* **37**, 428 (1966).
4. See, however, J. G. POWLES and J. H. STRANGE, *Proc. Phys. Soc.* **82** (1963); J. JEENER and P. BROEKAERT, *Phys. Rev.* **157**, 232 (1967).
5. A. ABRAGAM, "The Principles of Nuclear Magnetism," p. 120. Clarendon Press, Oxford, 1961.
6. D. C. LOOK, I. J. LOWE, and J. A. NORTHBY, *J. Chem. Phys.* **44**, 3441 (1966). D. E. BARNAAL and I. J. LOWE, *Phys. Rev.* **148**, 328 (1966), *J. Chem. Phys.* **46**, 4800 (1967).
7. D. E. BARNAAL, Thesis, University Minnesota (1965), University Microfilm #65-7867, and Ref. 6.
8. M. KOPP, Proceedings of the Second Materials Research Symposium, National Bureau of Standards, Washington, October 1967.
9. The Fortran Source Decks and User's Manual have been sent to Quantum Chemistry Program Exchange (Q.C.P.E.), Indiana University, Bloomington, Indiana.
10. M. KOPP and J. H. MACKEY, *J. Comp. Phys.* **3**, 539 (1969).
11. R. R. ERNST and W. A. ANDERSON, *Rev. Sci. Instr.* **37**, 93 (1966).
12. K. W. VOLLMERS, University of Pittsburgh, (private communication).